Published in final edited form as:
*Cell Rep*. 2017 February 07; 18(6): 1434–1443. doi:10.1016/j.celrep.2017.01.037.

# The CIA Targeting Complex Is Highly Regulated and Provides Two Distinct Binding Sites for Client Iron-Sulfur Proteins

**Diana C. Odermatt**[1] and **Kerstin Gari**[1,2,*]

[1]Institute of Molecular Cancer Research, University of Zurich, 8057 Zurich, Switzerland

## Summary

The cytoplasmic iron-sulfur assembly (CIA) targeting complex is required for the transfer of an iron-sulfur (Fe-S) cluster to cytoplasmic and nuclear proteins, but how it engages with client proteins is unknown. Here, we show that the complex members MIP18 and CIAO1 associate with the C terminus of MMS19. By doing so, they form a docking site for Fe-S proteins that is disrupted in the absence of either MMS19 or MIP18. The Fe-S helicase XPD seems to be the only exception, since it can interact with MMS19 independently of MIP18 and CIAO1. We further show that the direct interaction between MMS19 and MIP18 is required to protect MIP18 from proteasomal degradation. Taken together, these data suggest a remarkably regulated interaction between the CIA targeting complex and client proteins and raise the possibility that Fe-S cluster transfer is controlled, at least in part, by the stability of the CIA targeting complex itself.

## Introduction

MMS19/Mms19 was first identified in *Saccharomyces cerevisiae* as being methyl methanesulfonate sensitive (MMS) and required for the removal of UV-induced pyrimidine dimers (Prakash and Prakash, 1979). It was further shown to be involved in nucleotide excision repair (NER) and transcription (Lauder et al., 1996), which was later explained with its role in stabilizing the NER/transcription factor XPD (Kou et al., 2008).

In 2012, two studies reported that MMS19 is part of the cytoplasmic iron-sulfur assembly (CIA) machinery and, together with MIP18/FAM96B and CIAO1, is required for the transfer of an iron-sulfur (Fe-S) cluster to client Fe-S proteins (Gari et al., 2012; Lill et al., 2015; Stehling et al., 2012). Remarkably, many of its Fe-S client proteins are nuclear proteins with roles in DNA replication and repair, among them the NER/transcription factor XPD, and a number of DNA polymerases and helicases (Gari et al., 2012; Stehling et al., 2012). While



*Correspondence: gari@imcr.uzh.ch.
[2]Lead Contact

**Accession Numbers**

The accession number for the protein interactions reported in this paper and submitted to the IMEx Consortium (http://www.imexconsortium.org) through IntAct (Orchard et al., 2014) is IMEx: IM-25614.

**Author Contributions**

D.C.O. performed most experiments, with help from K.G., and contributed to writing the paper. K.G. supervised the work and wrote the manuscript.


Europe PMC Funders Author Manuscripts

the actual role of Fe-S clusters in the context of DNA metabolism is largely unknown, Fe-S cluster-binding mutant versions of these proteins are severely impaired in vitro and in vivo, indicating that Fe-S clusters are a prerequisite for proper protein function (Fuss et al., 2015; Netz et al., 2011; Rudolf et al., 2006; van der Lelij et al., 2010; Vashisht et al., 2015).

The finding that the levels of multiple Fe-S client proteins with roles in DNA replication and repair are severely affected in the absence of MMS19 (Gari et al., 2012; Stehling et al., 2012) provides a plausible explanation for MMS19's long-known, but elusive, role in the maintenance of genome stability. Moreover, reduced levels and/or activities of Fe-S proteins may also explain many, if not all, of the other phenotypes associated with loss of MMS19 (Ito et al., 2010; Kou et al., 2008; Li et al., 2011).

MMS19 contains several HEAT repeats, which are commonly involved in protein-protein interactions, but a thorough analysis on how MMS19 mediates binding to Fe-S proteins is still missing. Here we use co-immunoprecipitation (co-IP) experiments to show that CIA targeting complex members MIP18 and CIAO1 associate with the C-terminal HEAT repeats of MMS19 and, together, form a docking site for Fe-S proteins. With the exception of XPD that can directly interact with the N-terminal HEAT repeats of MMS19, all Fe-S proteins seem to require the presence of both MMS19 and MIP18 to bind to the CIA targeting complex. We further show that the direct interaction between MMS19 and the C terminus of MIP18 is required to protect MIP18 from proteasomal degradation, raising the possibility that Fe-S cluster incorporation into client proteins is regulated, at least in part, by the stability of the CIA targeting complex itself.

## Results

### MIP18 and CIAO1 Interact with the C Terminus of MMS19

HEAT repeats, as found in MMS19, are commonly involved in protein-protein interactions. To better understand the composition of the CIA targeting complex and the role of the HEAT repeats in MMS19, we generated truncation mutants of MMS19 (Figure 1A) comprising either the N-terminal HEAT repeats (fragment A), the central region (fragment B), or the C-terminal HEAT repeats (fragment C). Since we observed a very weak expression of fragment C (see Figure 1B, left panel, lanes 5 and 11), we included fragment D that contains the C-terminal HEAT repeats plus the central region. In pull-down (PD) experiments, we observed an association of MIP18 with full-length MMS19, as well as with fragments C and D (Figure 1B, right panel, lanes 2, 5, and 6), suggesting that MIP18 interacts with the C-terminal HEAT repeats of MMS19. When CIAO1 was included in the experiment, the interaction between MIP18 and the C-terminal HEAT repeats of MMS19 was strengthened, and we observed a trimeric complex (Figure 1B, right panel, lanes 11 and 12). In contrast, CIAO1 on its own displayed a very weak, if any, interaction with MMS19 (Figure 1C, right panel, lane 2). Taken together, these data suggest that MIP18 directly binds to the C-terminal HEAT repeats of MMS19, while CIAO1's interaction with MMS19 is primarily mediated by MIP18.

### MMS19 Interacts with the Extreme C Terminus of MIP18

We next wanted to define the binding site of MMS19 within MIP18. MIP18 has a domain of unknown function (DUF59) that is also found in the plant Fe-S scaffold protein HCF101 (Schwenkert et al., 2009). Outside of this domain, MIP18 seems to be little structured and is predicted to contain intrinsically disordered regions (IDRs) at both the N-terminal and C-terminal ends. Since disordered regions often feature protein interaction sites, we generated truncation mutants lacking either the N-terminal IDR (MIP18 ΔN1/2) or the C-terminal IDR (MIP18 ΔC) (Figure 2A) and checked them for their ability to bind to MMS19. While the N-terminal truncation mutants of MIP18 were proficient in binding to MMS19 when co-expressed, MIP18 ΔC displayed a dramatically reduced interaction with MMS19 (Figures 2B and 2D), suggesting that MMS19 binds to the C-terminal end of MIP18. On the other hand, MIP18 ΔC was able to bind to CIAO1 in the same way as full-length MIP18 (Figure 2C), ruling out the possibility that MIP18 ΔC was misfolded. Interestingly, co-expression of CIAO1 restored MIP18 ΔC binding to MMS19 (Figure 2D). This finding was rather surprising, given that MMS19 did not display any apparent interaction with either CIAO1 or MIP18 ΔC alone. We suspect that both CIAO1 and MIP18 ΔC bind weakly to MMS19 in a way that is barely detectable under our experimental conditions. However, in the presence of all complex partners, these weak interactions get stabilized.

### MIP18 Is Degraded by the Proteasome in the Absence of MMS19

In agreement with previously published data (Gari et al., 2012; Stehling et al., 2013), using five different small interfering RNAs (siRNAs) against MMS19, we observed that MIP18 protein levels were greatly reduced in the absence of MMS19 (Figure 3A). In contrast, MMS19 levels were similar in the presence or absence of MIP18 (Figure 3B). Taken together, these findings suggest a tight regulation of MIP18 rather than a reciprocal stabilization of the CIA complex partners. This notion was corroborated by the fact that *MIP18* overexpression was greatly increased when *MMS19* was co-expressed (Figure 3C, compare lanes 1 and 2), while *MMS19* overexpression levels did not change with concomitant expression of *MIP18* (see, for example, Figures 4A and 5A and 5B). Interestingly, the addition of the proteasome inhibitor MG132 increased MIP18 levels to the same extent as co-expression of *MMS19* (Figure 3C, compare lanes 1, 2, and 3), suggesting that the presence of MMS19 rescues MIP18 from proteasomal degradation.

To further understand how MIP18 levels are regulated, expression of *Flag-MIP18* was induced by the addition of doxycycline in cells that had either been treated with control siRNA or with siRNA directed against MMS19. The translation inhibitor cycloheximide (CHX) was added 4 hr after induction, and cells were harvested 0, 1, 6, and 22 hr after CHX treatment. The half-lives of both endogenous MIP18 and exogenous Flag-MIP18 were considerably shorter when MMS19 was absent (Figure 3D, upper panel). When the proteasome inhibitor MG132 was added together with CHX, MIP18/Flag-MIP18 levels were stabilized (Figure 3D, lower panel), further suggesting that the reduced MIP18 protein levels in the absence of MMS19 are due to proteasomal degradation. Interestingly, the degradation of MIP18 in the absence of MMS19 seems to be independent of ubiquitination, since mutating the five lysines in MIP18, either alone or in combination, did not result in a more stable version of MIP18 (data not shown).

### The Stability of MIP18 Depends on the Direct Interaction of MMS19 with Its C Terminus

We next wanted to address whether the direct interaction with MMS19 is a prerequisite for the protection of MIP18 from proteasomal degradation. To this end, we used the MIP18 truncation mutant MIP18 ΔC that displayed greatly reduced binding to MMS19 (Figures 2B and 2D). When the half-life of Flag-MIP18 ΔC was compared to full-length Flag-MIP18 in a similar setup as in Figure 3D, Flag-MIP18 ΔC was considerably less stable over time (Figure 3E), suggesting that the interaction with MMS19 is required for the protection of MIP18 from proteasomal degradation. In agreement with this notion, Flag-MIP18 ΔC levels were independent of the presence or absence of MMS19 (Figure 3F, upper panel) and were stabilized upon proteasomal inhibition (Figure 3F, lower panel). Taken together, these data suggest that MMS19 protects MIP18 from proteasomal degradation by directly binding to its C-terminal end.

### Interaction of the CIA Targeting Complex with the Fe-S Helicase XPD

We next wondered how the CIA targeting complex binds to Fe-S proteins and chose the Fe-S helicase XPD as a representative Fe-S protein. To this end, we performed co-IP experiments with Flag-MMS19 and XPD, and we observed a robust interaction between MMS19 and XPD (Figure 4A, right panel, lane 2) that was independent of the co-expression of MIP18 and/or CIAO1 (Figure 4A, right panel, lanes 2–5). We then investigated the binding of XPD to the above-described MMS19 truncation fragments. In addition to full-length MMS19, we also observed an interaction of XPD with fragment A (Figure 4B, right panel, lane 3), suggesting that XPD can bind to the N-terminal HEAT repeats of MMS19.

### Interaction of the CIA Targeting Complex with RTEL1 and DNA Polymerase Delta

Given that the CIA complex partners MIP18/CIAO1 associate with MMS19 via its C-terminal HEAT repeats, we wondered whether its N-terminal HEAT repeats could be a general docking site for Fe-S proteins. However, none of the other Fe-S proteins that were tested (namely, DNA polymerase delta [POLD1] and the Fe-S helicase RTEL1) were able to interact with the N-terminal HEAT repeats of MMS19 alone (data not shown). Moreover, both RTEL1 and DNA polymerase delta, in contrast to XPD, only interacted with MMS19 in the presence of both MIP18 and CIAO1 (Figures 5A and 5B, right panels).

We next wondered whether certain Fe-S proteins, such as DNA polymerase delta, were instead able to interact directly with MIP18 or CIAO1. However, when performing co-IP experiments with either Flag-MIP18 (Figure 5C) or Flag-CIAO1 (Figure S1), we again only observed binding of DNA polymerase delta when all three CIA targeting complex partners were co-expressed.

### XPD and DNA Polymerase Delta Display Different Interaction Modes with the CIA Targeting Complex

Our data thus far suggest that different binding modes to the CIA targeting complex exist, with XPD being able to directly interact with MMS19, while other Fe-S proteins, such as DNA polymerase delta and RTEL1, require the presence of all CIA targeting complex members. To further corroborate this notion, we performed pull-down experiments of Flag-tagged MMS19 in the presence or absence of MIP18 (cells treated with either control siRNA

or siRNA directed against MIP18). In agreement with our previous results, we observed binding of endogenous XPD to Flag-MMS19 both in the presence and absence of MIP18, while endogenous DNA polymerase delta only interacted with Flag-MMS19 in the presence of MIP18 (Figure 6A).

To address the possibility that Fe-S proteins interact differently with the CIA targeting complex in the absence of a functional Fe-S cluster maturation pathway (MMS19 or MIP18 knockdown) because they are misfolded or unstable, we tested how Fe-S cluster-binding mutant versions of XPD (C190S XPD) and DNA polymerase delta (C1076S POLD1) interact with MMS19, MIP18, and CIAO1 (Figure S2). While C190S XPD was expressed at much lower levels than wild-type XPD, underlining the structural role of the Fe-S cluster in XPD as shown by X-ray crystallography (Fan et al., 2008), it was still able to interact with MMS19, CIAO1, and MIP18 (Figure S2A). Interestingly, C1076S POLD1 appeared as stable as (if not more than) the wild-type protein and displayed a rather enhanced interaction with the CIA targeting complex (Figure S2B), excluding the possibility that the reduced interaction of DNA polymerase delta with Flag-MMS19 upon MIP18 knockdown (Figure 6A) was due to stability or folding issues.

## The Interaction of the Majority of Fe-S Proteins with the CIA Targeting Complex Depends on Both MMS19 and MIP18

To obtain a more general picture of how proteins bind to the CIA targeting complex, we used an unbiased mass spectrometry approach to test which proteins interact with Flag-MMS19 and Flag-MIP18 only in the presence of the partner protein (Figure 6B). To do so, Flag-MMS19 (siRNA control/MIP18) and Flag-MIP18 (siRNA control/MMS19) pull-down samples were subjected to mass spectrometry analysis, and the number of total peptides of all detected proteins was evaluated (Table S1). We then calculated the peptide ratio of siRNA MIP18 over the control sample (for the Flag-MMS19 PD) and siRNA MMS19 over the control sample (for the Flag-MIP18 PD), and we selected those proteins whose peptide ratios were below 33.3% (i.e., those proteins whose interaction with the bait protein was markedly reduced when the partner protein was knocked down). When only proteins that were below the threshold of 33.3% in both experimental repeats were considered, the list of proteins for each pull-down experiment was relatively short and the two lists showed a considerable overlap (Figure S3A). We next cross-checked all proteins that were found to be below the threshold in one of the pull-down experiments for their peptide ratio in the other pull-down experiment (Figure S3B). All proteins whose peptide ratios (knockdown over control) were below the threshold in one pull-down experiment (both experimental repeats) and below the threshold in at least one of the two experimental repeats of the other pull-down experiment are shown in Figure 6C.

Only six proteins were found to be below the threshold in both experimental repeats of both pull-down experiments—namely, CDKAL, DNA polymerase delta (DPOD1), the large subunit of DNA primase (PRI2), amidophosphoribosyltransferase (PUR1), 4-demethylwyosine synthase (TYW1), and CSE1L/Exportin-2 (XPO2). Remarkably, with the exception of CSE1L, which has not been associated with Fe-S clusters before, all proteins are known Fe-S proteins. Moreover, among the four proteins whose interaction with Flag-

MMS19/MIP18 in the absence of the partner protein was reduced in three of four experiments, we found another Fe-S protein (RTEL1), as well as two proteins that are part of a complex that contains an Fe-S protein: the small subunit of DNA primase (PRI1) that is in complex with PRI2, and ELP1 that is found in complex with the Fe-S protein ELP3.

Taken together, these results show that knockdown of MIP18 or MMS19 appears to selectively reduce the interaction of the CIA targeting complex with Fe-S proteins, suggesting that MMS19 and MIP18, together, form a docking site for Fe-S proteins. The notable exception seems to be XPD that can interact with MMS19 independently of MIP18 (Figures 4, 6A, and S3B). It remains to be determined whether XPD binds to MMS19 in a way that differs from other Fe-S proteins or whether it has two interaction sites with MMS19: one with the N-terminal HEAT repeats, and one with the C terminus of MMS19 in conjunction with MIP18 and CIAO1, as observed for other Fe-S proteins.

## Discussion

While the importance of the CIA targeting complex for Fe-S cluster transfer to DNA replication and repair proteins was described previously (Gari et al., 2012; Stehling et al., 2012, 2013), complex arrangement and mode of interaction with Fe-S proteins remained largely unclear. Here we provide evidence that MIP18 and CIAO1 interact with the C-terminal HEAT repeats of MMS19 to form a docking site for Fe-S proteins.

Our co-IP data suggest a direct binding of MIP18 to the C-terminal HEAT repeats of MMS19 (Figure 1B). While a direct interaction between MMS19 and MIP18 is supported by a study from 2013 using purified proteins (Seki et al., 2013), no interaction between MMS19 and MIP18 was observed when using in vitro translated proteins (van Wietmarschen et al., 2012). Although we cannot know for certain, we suspect that in vitro translated MMS19 and/or MIP18 (van Wietmarschen et al., 2012) might not fold properly and hence displays altered binding behavior.

Our data (Figures 1C, 4A, and 5A and 5B) further suggest that CIAO1 requires the presence of MIP18 for a stable interaction with MMS19. Without structural analysis of the CIA targeting complex, it is difficult to say whether the interaction between MMS19 and CIAO1 is solely mediated by MIP18, as suggested previously (Seki et al., 2013), or whether CIAO1 displays a weak affinity for MMS19 that is greatly enhanced by MIP18. Since we observe that CIAO1 and the MMS19-binding mutant MIP18 ΔC can together form a complex with MMS19, while they do not display any obvious binding to MMS19 when tested individually, we favor the interpretation that CIAO1 can weakly bind to MMS19.

We further show that MIP18 protein stability depends on the presence of MMS19 (Figures 3A, 3C, and 3D) and on its direct interaction with MMS19 (Figure 3E). While it is not uncommon that proteins get targeted for proteasomal degradation in the absence of their complex partner to avoid the accumulation of unnecessary proteins, it is striking to notice that MMS19 in turn is perfectly stable without MIP18 (Figure 3B).

Apart from a purely housekeeping function, the tight regulation of MIP18 may also serve the purpose of limiting the formation of non-productive interactions between the CIA targeting

complex and Fe-S proteins at times when Fe-S cluster transfer cannot take place. In agreement with this notion, our data suggest that a DNA polymerase delta mutant that is deficient for Fe-S cluster binding displays an enhanced (presumably non-productive) interaction with the CIA targeting complex (Figure S2B), possibly because release from the complex requires the functional transfer of an Fe-S cluster. Alternatively (or additionally), the tight regulation of MIP18 may also be a way to control or limit Fe-S cluster transfer. We speculate that unscheduled Fe-S incorporation into Fe-S client proteins may be harmful to the cell and, hence, restricted as much as possible.

Interestingly, our study suggests that the majority of Fe-S proteins bind to the CIA targeting complex only in the presence of all three complex proteins MMS19, MIP18, and CIAO1. The most straightforward interpretation of this finding is that MMS19, MIP18, and CIAO1, conjointly, form a docking site for Fe-S client proteins. However, we cannot exclude that the formation of the ternary complex induces a conformational change in one of the proteins that exposes an interaction site for Fe-S proteins that would not be accessible otherwise. Further structural studies will have to clarify which domains/proteins of the complex are in direct physical contact with Fe-S proteins. In any case, such a concerted binding mode that requires the presence of at least three proteins further points toward a tight regulation of Fe-S cluster transfer.

Unexpectedly, the Fe-S helicase XPD displayed a different binding mode to MMS19 than other Fe-S proteins. Our co-IP (Figures 4 and 6A) and mass spectrometry (Figure S3B) data collectively suggest that XPD binds to the N-terminal HEAT repeats of MMS19 independently of MIP18 and CIAO1. Hence, it appears that XPD may be the odd one out that binds to the CIA targeting complex, and receives an Fe-S cluster, in a way that is different from other Fe-S proteins. It should be added, however, that we did not detect all Fe-S proteins that are known to interact with the CIA targeting complex in our mass spectrometry analysis. Thus, we cannot exclude that other Fe-S proteins display behaviors similar to XPD.

Another possibility is that XPD features two interaction sites with the CIA targeting complex: one with the N terminus of MMS19 and one with the “canonical” Fe-S docking site at the C terminus of MMS19 that depends on MIP18 and CIAO1. In agreement with this possibility, the interaction of XPD with Flag-MMS19 appears slightly reduced in the absence of MIP18 (Figures 6A and S3B). In a hypothetical scenario (Figure 7), XPD would bind to the Fe-S docking site at the C terminus of MMS19 in the same way as other Fe-S proteins to receive an Fe-S cluster. XPD binding to the N-terminal HEAT repeats of MMS19, on the other hand, may serve a purpose other than Fe-S cluster transfer.

In this context, it should be noted that a role for the so-called MMXD complex (composed of MMS19, MIP18, and XPD) in chromosome segregation was suggested previously (Ito et al., 2010). To date, however, it has remained unclear whether the role of MMS19 in this context is direct or rather indirect due to its impact on XPD stability and possibly the stability of other Fe-S proteins with roles in chromosome segregation, such as the related helicase ChlR1 (van der Lelij et al., 2010). A second interaction site of XPD with MMS19,

in addition to a binding site whose sole purpose is the transfer of an Fe-S cluster, may be suggestive of additional roles of MMS19 in conjunction with XPD.

Interestingly, while Fe-S cluster transfer was found to precede the functional integration of XPD into transcription factor IIH (Vashisht et al., 2015), our mass spectrometry data suggest that this is not the case for DNA primase assembly (Figure 6C). The fact that both subunits of DNA primase (PRI1/2) are found in our pull-down experiments, and that their interaction with the CIA targeting complex seems to depend on the presence of both MMS19 and MIP18, suggests that the complex forms prior to Fe-S cluster incorporation into PRI2. Hence, in contrast to XPD, the Fe-S cluster in DNA primase does not seem to be required for the interaction between the subunits and for hetero-complex formation. This may also suggest that the Fe-S cluster in DNA primase has less of a structural role than the Fe-S cluster in XPD, which is required for folding of the Fe-S domain (Fan et al., 2008).

## Experimental Procedures

### Cell Lines

HEK293T and human cervix epithelioid carcinoma (HeLa) cells were cultured in DMEM containing 10% fetal calf serum (FCS). Parental HeLa Flp-In T-REx (Tighe et al., 2008) cells were cultured in DMEM containing 10% FCS supplemented with 15 μg/mL Blasticidin and 100 μg/mL Zeocin. After integration of expression constructs, the medium was supplemented with 15 μg/mL Blasticidin and 150 μg/mL Hygromycin (all reagents were from Invitrogen/Thermo Fisher Scientific).

### Plasmids and Transfection in Human Cells

All plasmids were based on the GATEWAY system (Invitrogen). GATEWAY destination vectors used in transfections allowed expression of either untagged, Flag-tagged, or myc-tagged constructs under the control of a cytomegalovirus (CMV) promoter.

Transient plasmid transfections were performed in HEK293T cells using calcium phosphate transfection. Briefly, 293T cells were seeded 1:5 the day prior to transfection. On the day of transfection, 5 μg of each plasmid was diluted in $H_2O$ to a final volume of 450 μL, and then 50 μL 2.5 M $CaCl_2$ was added. The plasmid DNA/$CaCl_2$ mix was then added drop-wise to 500 μL 2× HBS (HEPES-buffered saline; 280 mM NaCl, 50 mM HEPES, and 1.5 mM $Na_2HPO_4$, pH 7.05). The medium was replaced with FCS-free medium, and the transfection mix was added drop-wise to the cells. After 6 hr, the medium was changed to normal growth medium, and cells were harvested 48 hr after transfection.

HeLa Flp-In T-REx cell lines expressing the gene of interest were generated by co-transfecting a Flp-In-compatible expression vector with a plasmid coding for Flp recombinase (pOG44) using Lipofectamine 2000 (Thermo Fisher Scientific) according to the manufacturer's protocol. Expression of constructs was induced by the addition of 1 μg/mL doxycycline 48 hr before the cells were harvested, unless stated otherwise.

### siRNA Transfection

Control siRNA (5′-AGGUAGUGUAAUCGCCUUG), siRNA MMS19 number 1 (5′-AGAA GAGACUGGUGCGCAA), siRNA MMS19 number 2 (5′-GCAA CUAUACAGUGUU ACA), siRNA MMS19 number 3 (5′-ACCUGAUACUGUU CUAUGA), siRNA MMS19 number 4 (5′-GGCUGUUUCUGUGCUUAAA), siRNA MMS19 number 5 (5′-GCAAUGUACU GCCUUUACU), siRNA MIP18 number 1 (5′-ACAAGCAACUUGCAGAUAA), and siRNA MIP18 number 2 (5′-UUAUUGGUCUGUCCAUCAA) were purchased from Microsynth. siRNAs were transfected using Dharmafect 1 (Thermo Fisher Scientific) according to the manufacturer's protocol. After the first transfection (day 1), cells were split and re-transfected on day 4. Unless stated otherwise, knockdowns of MMS19 and MIP18 were usually done using siRNA number 1.

### Antibodies Used for Western Blotting

The following antibodies were used for western blotting: β-actin-horseradish peroxidase (HRP) (C4, sc-47778; Santa Cruz Biotechnology), CIAO1 (ab83088; Abcam), Flag-M2, clone M2 (F1804; Sigma-Aldrich), MIP18/FAM96B (20108-1-AP; Proteintech), MMS19 (16015-1-AP; Proteintech), c-*myc* (A00704-100; Genescript), polymerase delta catalytic subunit (ab10362; Abcam), and XPD (ab54676; Abcam).

### Preparation of Cell Extracts and Immunoprecipitation Experiments

Whole cell extracts (WCEs) were prepared using 3 packed cell volumes (PCVs) of buffer A containing 50 mM $Na_2HPO_4/NaH_2PO_4$ (pH 7.4), 150 mM NaCl, 10% glycerol, 0.1% NP-40, 0.5 mM EDTA, 1 mM TCEP (Tris[2-carboxyethyl]phosphine), and protease inhibitors. After incubation on ice for 30 min, the samples were spun at 13,000 rpm and 4°C for 30 min. For pull-down experiments, extracts were incubated overnight on Flag-M2 beads (Sigma-Aldrich) at 4°C. The following day, the supernatant was removed and the beads were washed extensively with buffer A. Bound proteins were eluted in buffer A containing 200 μg/mL 3× Flag peptide (Sigma-Aldrich) for 1 hr at 4°C. Protein-protein interactions were analyzed by SDS-PAGE and western blotting.

### Time Course of Protein Stability

HeLa Flp-In T-REx cells inducibly expressing Flag-MIP18 or Flag-MIP18 ΔC were treated twice with the indicated siRNAs (days 1 and 4). On day 5, protein expression was induced by the addition of doxycycline. After 4 hr, 100 μg/mL cycloheximide either with or without 10 μg/mL MG132 was added, and cells were collected at various time points (0, 1, 3, 6, and 22 hr after drug addition).

### Preparation of Cytoplasmic Extracts for Mass Spectrometry

HeLa Flp-In T-REx cells inducibly expressing Flag-MMS19 or Flag-MIP18 were treated twice with the indicated siRNAs (days 1 and 4). On day 5, protein expression was induced by addition of doxycycline for 24 hr. To overcome the limitations of MIP18 instability in the absence of MMS19, cells were treated with 10 μg/mL MG132 6 hr prior to collection in experiments using siRNA directed against MMS19. For the preparation of cytoplasmic

extracts, the cytoplasmic membrane was lysed with 5 PCVs of buffer B (20 mM $Na_2HPO_4/NaH_2PO_4$ [pH 7.0], 10 mM NaCl, 0.5 mM EDTA, 0.5% NP-40, 1 mM TCEP, and protease inhibitors) for 20 min on a rotating wheel at 4°C. An equal volume of buffer C (50 mM $Na_2HPO_4/NaH_2PO_4$ [pH 7.0], 290 mM NaCl, 12.5% glycerol, 0.5 mM EDTA, 1 mM TCEP, and protease inhibitors) was added, and the samples were spun for 20 min at 4,000 rpm and 4°C. The supernatants were then subjected to another centrifugation round at 13,000 rpm and 4°C for 30 min to remove residual debris. Extracts were incubated overnight on Flag-M2 beads at 4°C. The following day, the supernatant was removed, the beads were washed extensively with buffer A (pH 7.0), and bound proteins were eluted in buffer D (50 mM $Na_2HPO_4/NaH_2PO_4$ [pH 7.0], 150 mM NaCl, 10% glycerol, 0.01% NP-40, 0.5 mM EDTA, 1 mM TCEP, and 200 μg/mL 3× Flag peptide) for 1 hr at 4°C. Interactions were analyzed by mass spectrometry.

### Mass Spectrometry

Samples were precipitated with an equal volume of 20% trichloroacetic acid (TCA; Sigma-Aldrich) and washed twice with cold acetone. The dry pellets were dissolved in 45 μL buffer (10 mM Tris [pH 8.2], 2 mM $CaCl_2$) and 5 μL trypsin (100 ng/μL in 10 mM HCl) for digestion, which was carried out in a microwave instrument (Discover System; CEM) for 30 min at 5 W and 60°C. Samples were dried in a SpeedVac (Savant). For liquid chromatography (LC)-tandem mass spectrometry (MS/MS) analysis, the samples were dissolved in 0.1% formic acid (Romil) and an aliquot ranging from 5% to 25% was analyzed on a nanoAcquity UPLC System (Waters) connected to a Q Exactive mass spectrometer (Thermo Scientific) equipped with a Digital PicoView source (New Objective). Peptides were trapped on a Symmetry C18 trap column (5 μm, 180 μm × 20 mm; Waters) and separated on a BEH300 C18 column (1.7 μm, 75 μm × 150 m; Waters) at a flow rate of 250 nL/min using a gradient from 1% solvent B (0.1% formic acid in acetonitrile; Romil)/99% solvent A (0.1% formic acid in water; Romil) to 40% solvent B/60% solvent A within 90 min. Mass spectrometry settings for the data-dependent analysis were as follows: (1) precursor scan range, mass-to-charge ratio (m/z) of 350–1,500; resolution, 70,000; maximum injection time, 100 ms; and threshold, 3e6; and (2) fragment ion scan range, 200–2,000 m/z; resolution, 35,000; maximum injection time, 120 ms; and threshold, 1e5.

Proteins were identified using the Mascot search engine (version 2.4.1; Matrix Science). Mascot was set up to search the Swiss-Prot database assuming the digestion enzyme trypsin. Mascot was searched with a fragment ion mass tolerance of 0.030 Da and a parent ion tolerance of 10.0 ppm. Oxidation of methionine was specified in Mascot as a variable modification. Scaffold (Proteome Software) was used to validate MS/MS-based peptide and protein identifications. Peptide identifications were accepted if they achieved a false discovery rate (FDR) of less than 0.1% by the scaffold local FDR algorithm. Protein identifications were accepted if they achieved an FDR of less than 1.0% and contained at least two identified peptides.

## Supplementary Material

Refer to Web version on PubMed Central for supplementary material.

## Acknowledgments

We thank Stephen S. Taylor for providing HeLa Flp-In T-REx cells, and we also thank Peter Hunziker and the Functional Genomics Center Zurich for mass spectrometry analyses. This work was supported by the Swiss National Science Foundation (SNSF) (professorship PP00P3_144784/1), the Human Frontier Science Program (HFSP) (career development award CDA00043/2013-C), and the University of Zurich.

## References

Fan L, Fuss JO, Cheng QJ, Arvai AS, Hammel M, Roberts VA, Cooper PK, Tainer JA. XPD helicase structures and activities: insights into the cancer and aging phenotypes from XPD mutations. Cell. 2008; 133:789–800. [PubMed: 18510924]

Fuss JO, Tsai CL, Ishida JP, Tainer JA. Emerging critical roles of Fe-S clusters in DNA replication and repair. Biochim Biophys Acta. 2015; 1853:1253–1271. [PubMed: 25655665]

Gari K, León Ortiz AM, Borel V, Flynn H, Skehel JM, Boulton SJ. MMS19 links cytoplasmic iron-sulfur cluster assembly to DNA metabolism. Science. 2012; 337:243–245. [PubMed: 22678361]

Ito S, Tan LJ, Andoh D, Narita T, Seki M, Hirano Y, Narita K, Kuraoka I, Hiraoka Y, Tanaka K. MMXD, a TFIIH-independent XPD-MMS19 protein complex involved in chromosome segregation. Mol Cell. 2010; 39:632–640. [PubMed: 20797633]

Kou H, Zhou Y, Gorospe RMC, Wang Z. Mms19 protein functions in nucleotide excision repair by sustaining an adequate cellular concentration of the TFIIH component Rad3. Proc Natl Acad Sci USA. 2008; 105:15714–15719. [PubMed: 18836076]

Lauder S, Bankmann M, Guzder SN, Sung P, Prakash L, Prakash S. Dual requirement for the yeast MMS19 gene in DNA repair and RNA polymerase II transcription. Mol Cell Biol. 1996; 16:6783–6793. [PubMed: 8943333]

Li F, Martienssen R, Cande WZ. Coordination of DNA replication and histone modification by the Rik1-Dos2 complex. Nature. 2011; 475:244–248. [PubMed: 21725325]

Lill R, Dutkiewicz R, Freibert SA, Heidenreich T, Mascarenhas J, Netz DJ, Paul VD, Pierik AJ, Richter N, Stümpfig M, et al. The role of mitochondria and the CIA machinery in the maturation of cytosolic and nuclear iron-sulfur proteins. Eur J Cell Biol. 2015; 94:280–291. [PubMed: 26099175]

Netz DJA, Stith CM, Stümpfig M, Köpf G, Vogel D, Genau HM, Stodola JL, Lill R, Burgers PMJ, Pierik AJ. Eukaryotic DNA polymerases require an iron-sulfur cluster for the formation of active complexes. Nat Chem Biol. 2011; 8:125–132. [PubMed: 22119860]

Orchard S, Ammari M, Aranda B, Breuza L, Briganti L, Broackes-Carter F, Campbell NH, Chavali G, Chen C, del-Toro N, et al. The MIntAct project–IntAct as a common curation platform for 11 molecular interaction databases. Nucleic Acids Res. 2014; 42:D358–D363. [PubMed: 24234451]

Prakash L, Prakash S. Three additional genes involved in pyrimidine dimer removal in Saccharomyces cerevisiae: RAD7, RAD14 and MMS19. Mol Gen Genet. 1979; 176:351–359. [PubMed: 392238]

Rudolf J, Makrantoni V, Ingledew WJ, Stark MJR, White MF. The DNA repair helicases XPD and FancJ have essential iron-sulfur domains. Mol Cell. 2006; 23:801–808. [PubMed: 16973432]

Schwenkert S, Netz DJA, Frazzon J, Pierik AJ, Bill E, Gross J, Lill R, Meurer J. Chloroplast HCF101 is a scaffold protein for [4Fe-4S] cluster assembly. Biochem J. 2009; 425:207–214. [PubMed: 19817716]

Seki M, Takeda Y, Iwai K, Tanaka K. IOP1 protein is an external component of the human cytosolic iron-sulfur cluster assembly (CIA) machinery and functions in the MMS19 protein-dependent CIA pathway. J Biol Chem. 2013; 288:16680–16689. [PubMed: 23585563]

Stehling O, Vashisht AA, Mascarenhas J, Jonsson ZO, Sharma T, Netz DJ, Pierik AJ, Wohlschlegel JA, Lill R. MMS19 assembles iron-sulfur proteins required for DNA metabolism and genomic integrity. Science. 2012; 337:195–199. [PubMed: 22678362]

Stehling O, Mascarenhas J, Vashisht AA, Sheftel AD, Niggemeyer B, Rösser R, Pierik AJ, Wohlschlegel JA, Lill R. Human CIA2A-FAM96A and CIA2B-FAM96B integrate iron homeostasis and maturation of different subsets of cytosolic-nuclear iron-sulfur proteins. Cell Metab. 2013; 18:187–198. [PubMed: 23891004]

Tighe A, Staples O, Taylor S. Mps1 kinase activity restrains anaphase during an unperturbed mitosis and targets Mad2 to kinetochores. J Cell Biol. 2008; 181:893–901. [PubMed: 18541701]

van der Lelij P, Chrzanowska KH, Godthelp BC, Rooimans MA, Oostra AB, Stumm M, Zdzienicka MZ, Joenje H, de Winter JP. Warsaw breakage syndrome, a cohesinopathy associated with mutations in the XPD helicase family member DDX11/ChlR1. Am J Hum Genet. 2010; 86:262–266. [PubMed: 20137776]

van Wietmarschen N, Moradian A, Morin GB, Lansdorp PM, Uringa E-J. The mammalian proteins MMS19, MIP18, and ANT2 are involved in cytoplasmic iron-sulfur cluster protein assembly. J Biol Chem. 2012; 287:43351–43358. [PubMed: 23150669]

Vashisht AA, Yu CC, Sharma T, Ro K, Wohlschlegel JA. The association of the Xeroderma pigmentosum group D DNA helicase (XPD) with transcription factor IIH is regulated by the cytosolic iron-sulfur cluster assembly pathway. J Biol Chem. 2015; 290:14218–14225. [PubMed: 25897079]



Europe PMC Funders Author Manuscripts

Europe PMC Funders Author Manuscripts

## Highlights

- MMS19, MIP18, and CIAO1 form a docking site for Fe-S proteins
- The Fe-S helicase XPD interacts independently and directly with MMS19
- MMS19 binds to MIP18 and protects it from proteasomal degradation

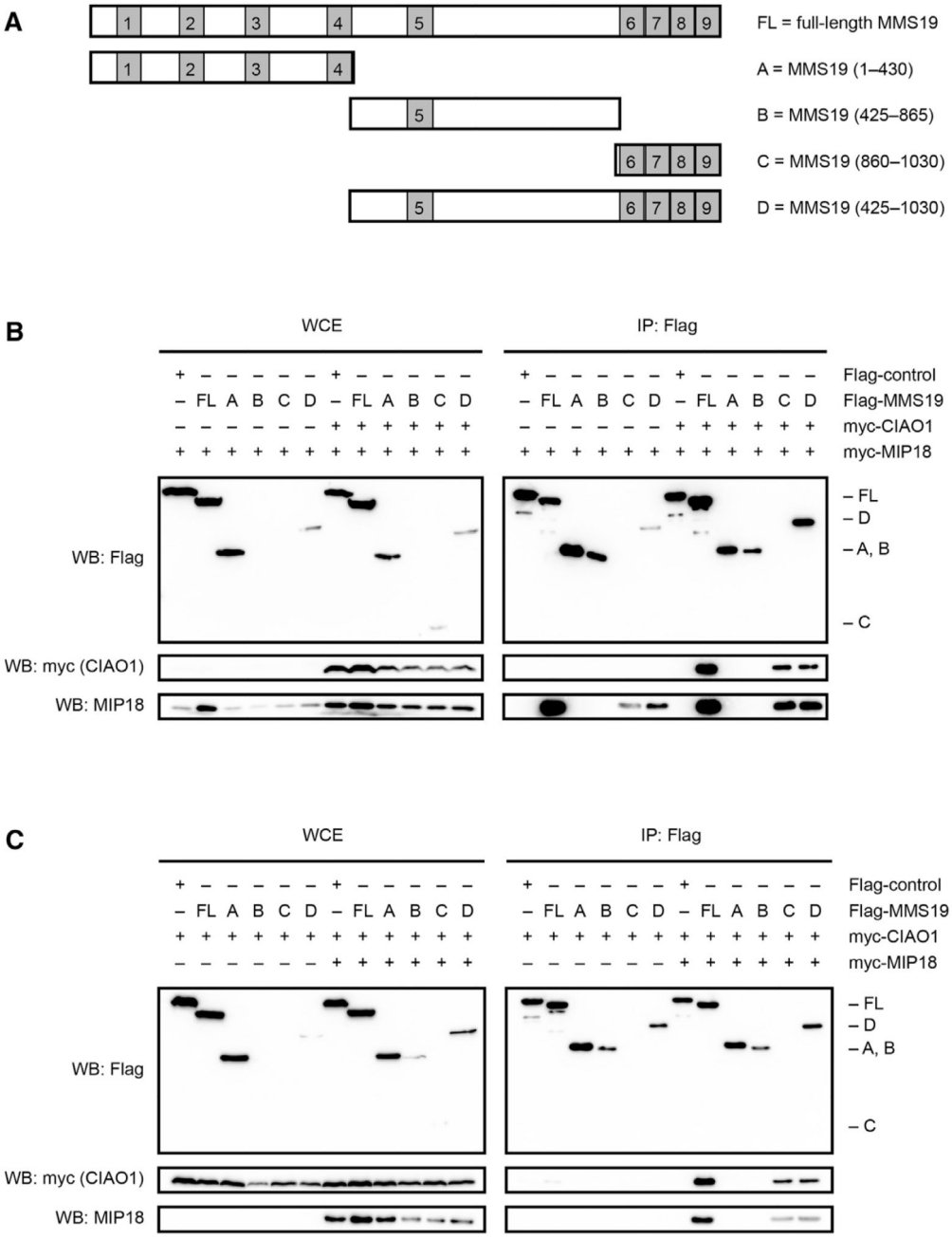


**Figure 1. MIP18 and CIAO1 Associate with MMS19 via Its C-Terminal HEAT Repeats**

(A) MMS19 fragments used. HEAT repeats are depicted in light gray and numbered 1–9. Amino acids encompassed in the fragments are shown in brackets.

(B) Co-expression and co-IP of Flag-MMS19 fragments with myc-MIP18 with or without myc-CIAO1. WB, western blot; WCE, whole cell extract.

(C) Co-expression and co-IP of Flag-MMS19 fragments with myc-CIAO1 with or without myc-MIP18.




Europe PMC Funders Author Manuscripts

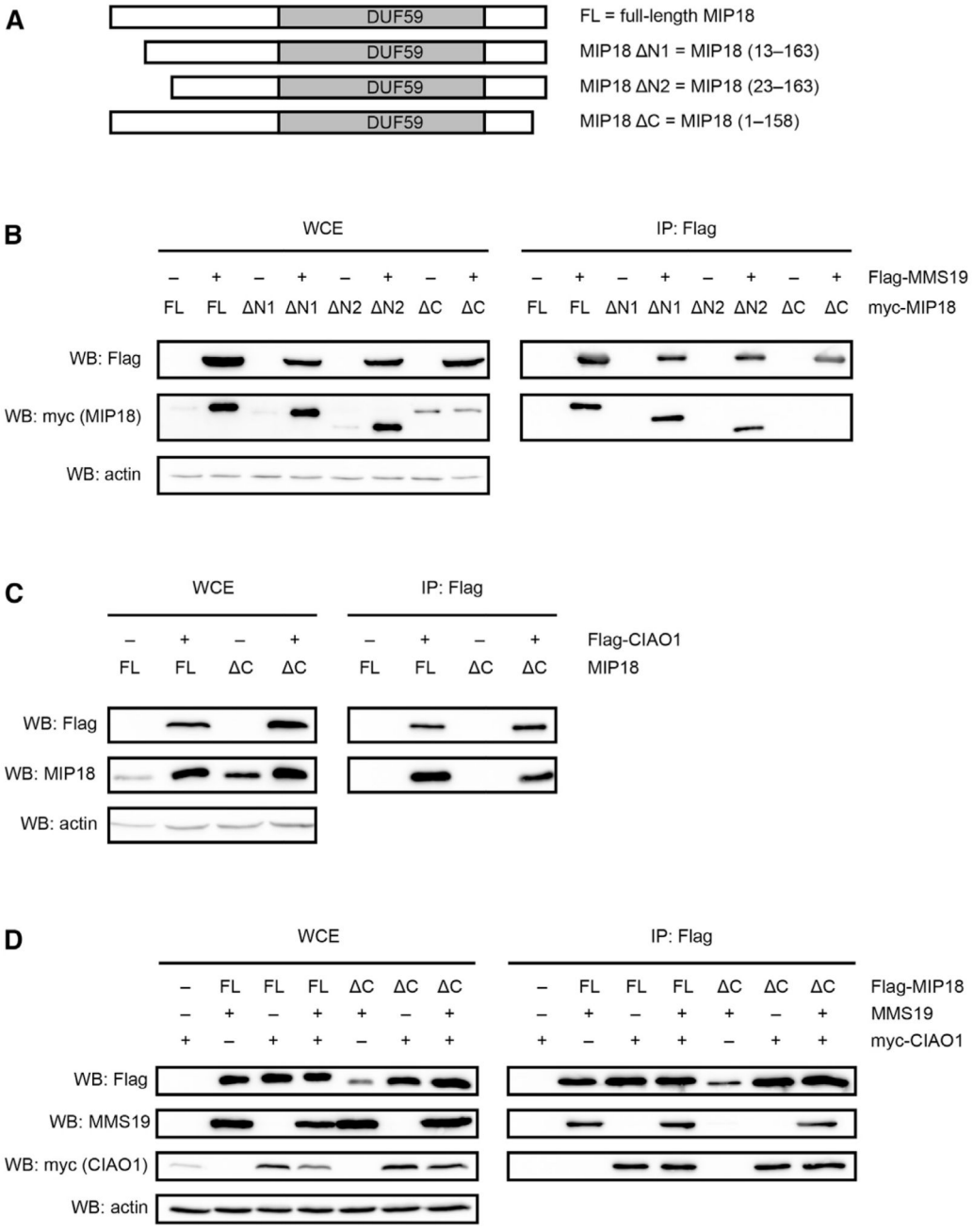


**Figure 2. MMS19 Binds to MIP18 at Its C-Terminal End**

(A) MIP18 fragments used. The DUF59 domain is depicted in light gray.

(B) Co-expression and co-IP of Flag-tagged MMS19 with full-length MIP18 or with N-terminal (MIP18 ΔN1/2) or C-terminal (MIP18 ΔC) truncation mutants of MIP18.

(C) Co-expression and co-IP of Flag-tagged CIAO1 with MIP18 or MIP18 ΔC.

(D) Co-expression and co-IP of Flag-tagged MIP18 or MIP18 ΔC with MMS19 and/or CIAO1.

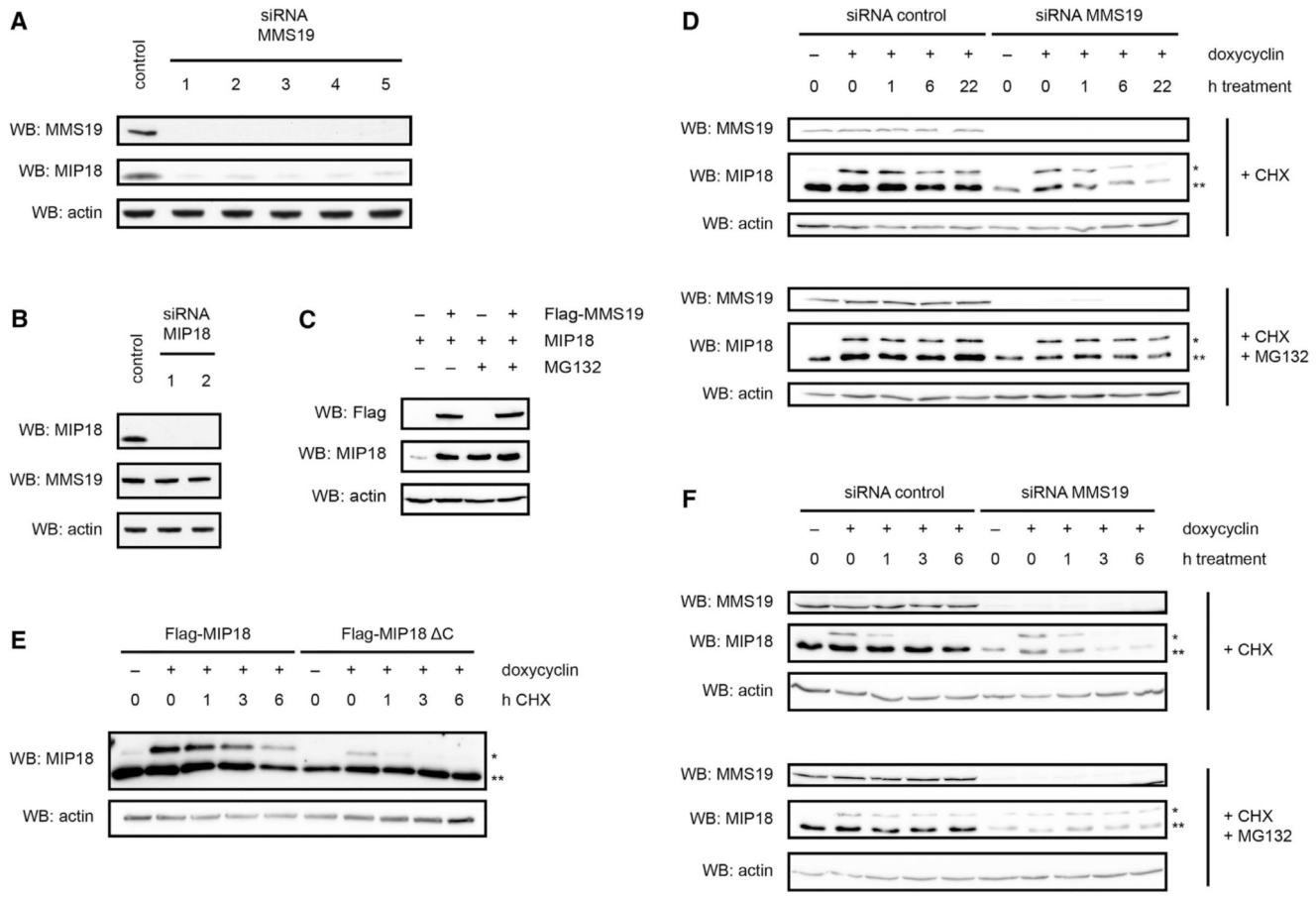


**Figure 3. MIP18 Is Targeted for Degradation by the Proteasome in the Absence of MMS19**

(A) Knockdown of MMS19 in HeLa cells using five different siRNAs (numbers 1–5) results in reduced MIP18 protein levels in WCEs.

(B) Knockdown of MIP18 in HeLa cells using two different siRNAs (numbers 1 and 2) does not affect MMS19 protein levels in WCEs.

(C) Expression of MIP18 with or without co-expression of Flag-MMS19 in the absence or presence of the proteasomal inhibitor MG132.

(D) Time course analysis of the stability of inducibly expressed Flag-MIP18 upon addition of the translation inhibitor CHX in the presence (siRNA control) or absence (siRNA MMS19) of MMS19, and without (upper panel) or with (lower panel) MG132.

(E) Time course analysis of the stability of inducibly expressed Flag-MIP18 and Flag-MIP18 ΔC upon addition of CHX.

(F) Time course analysis of the stability of Flag-MIP18 ΔC upon addition of CHX in the presence (siRNA control) or absence (siRNA MMS19) of MMS19, and without (upper panel) or with (lower panel) MG132. The single asterisks indicate Flag-tagged MIP18 or MIP18 ΔC, whereas the double asterisks indicate endogenous MIP18.

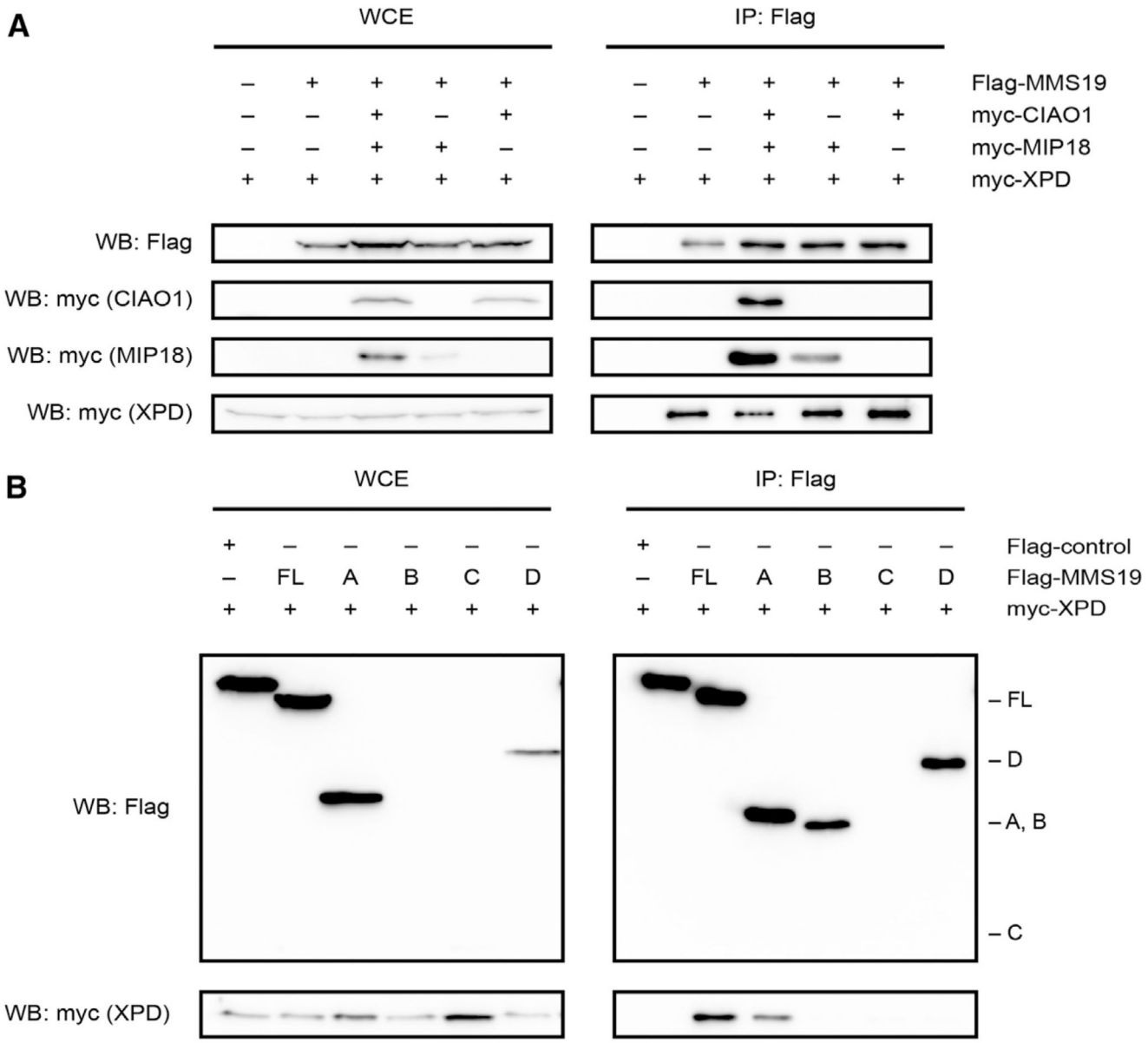


**Figure 4. The Fe-S Helicase XPD Interacts with the N-Terminal HEAT Repeats of MMS19 Independently of MIP18 and CIAO1**

(A) Co-expression and co-IP of Flag-MMS19 with myc-XPD in the presence or absence of myc-MIP18 and/or myc-CIAO1.

(B) Co-expression and co-IP of Flag-MMS19 fragments with myc-XPD.




Europe PMC Funders Author Manuscripts

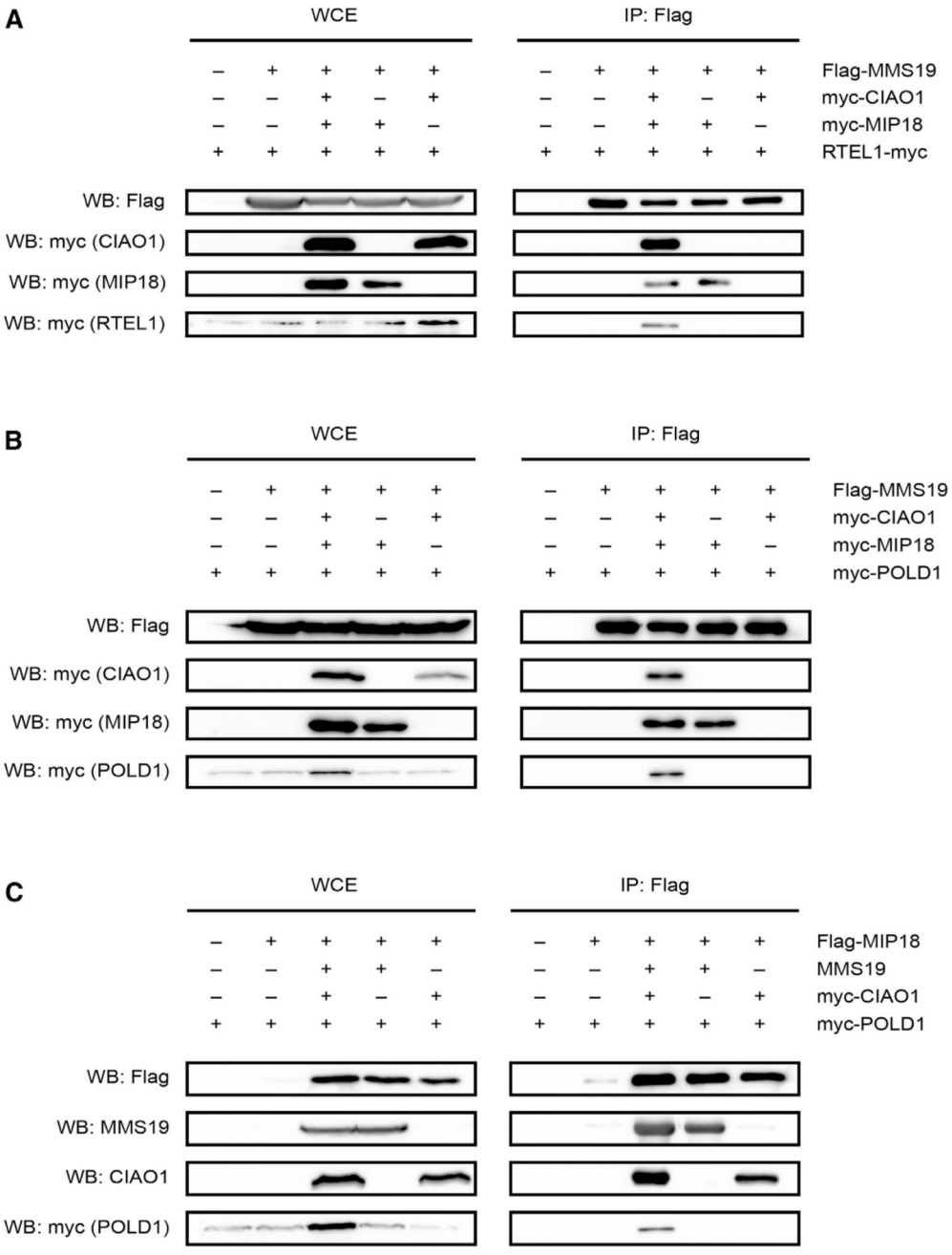


**Figure 5. The Interaction of RTEL1 and DNA Polymerase Delta with the CIA Targeting Complex Depends on MMS19, MIP18, and CIAO1**

(A and B) Co-expression and co-IP of Flag-MMS19 with RTEL1-myc (A) or myc-POLD1 (B) with or without concomitant overexpression of myc-MIP18 and/or myc-CIAO1.

(C) Co-expression and co-IP of Flag-MIP18 with myc-POLD1 with or without concomitant overexpression of MMS19 and/or myc-CIAO1.

See also Figure S1.

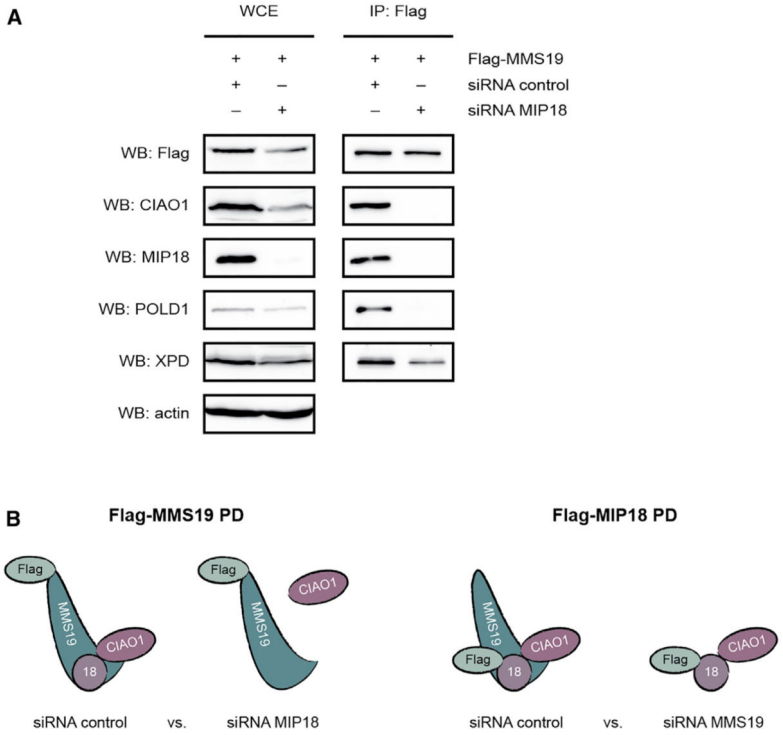


C

| | Flag-MMS19 PD si18/siC ratio (%) | Flag-MIP18 PD si19/siC ratio (%) | Comments |
|---|---|---|---|
| **CDKAL** | **17** | **18** | **FeS protein** |
| **DPOD1** | **2** | **0** | **FeS protein** |
| EDC4 | ND/0 | 0 | |
| ELP1 | ND/0 | 0 | in complex with FeS protein (ELP3) |
| PRI1 | 0 | 0/ND | in complex with FeS protein (PRI2) |
| **PRI2** | **5** | **0** | **FeS protein** |
| **PUR1** | **0** | **0** | **FeS protein** |
| **RTEL1** | **0** | **0/ND** | **FeS protein** |
| **TYW1** | **0** | **0** | **FeS protein** |
| XPO2 | 15 | 0 | |

**Colour code:**

| |
|---|
| below threshold in both PDs (one PD: both duplicates; other PD: only one of the duplicates) |
| below threshold in both PDs (both duplicates each) |

**Figure 6. The Interaction of the Majority of Fe-S Proteins with the CIA Targeting Complex Depends on Both MMS19 and MIP18**

(A) Immunoprecipitation (IP) of inducibly expressed Flag-MMS19 in the presence (siRNA control) or absence (siRNA MIP18) of MIP18 and western blot analysis of endogenous CIA complex partners or Fe-S proteins.

(B) Scheme of mass spectrometry analysis of Flag-MMS19 interaction partners in the presence (siRNA control) or absence (siRNA MIP18) of MIP18, and Flag-MIP18 interaction partners in the presence (siRNA control) or absence (siRNA MMS19) of MMS19.

(C) List of proteins whose interaction with Flag-MMS19 or Flag-MIP18 was markedly reduced in the absence of the partner protein. Shown are total peptide ratios of siRNA MIP18 over control or siRNA MMS19 over control samples (numbers represent the average ratio of two experimental repeats). ND, not detected; si18, siRNA against MIP18; si19, siRNA against MMS19; siC, control siRNA.
See also Figures S2 and S3 and Table S1.



Europe PMC Funders Author Manuscripts

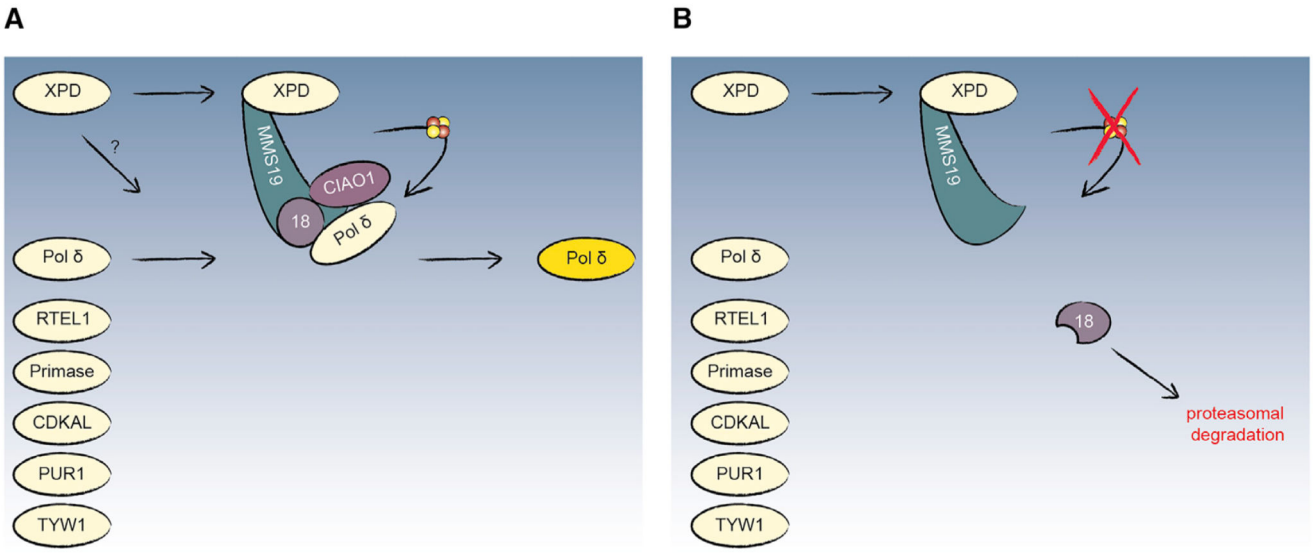


**Figure 7. Model**

(A) MIP18 and CIAO1 interact with the C-terminal HEAT repeats of MMS19 and form a docking site for Fe-S proteins to bind to and Fe-S cluster transfer to occur. In contrast to other Fe-S proteins, XPD can interact with the N-terminal HEAT repeats of MMS19 independently of MIP18 and CIAO1. It may or may not associate with the C terminus of MMS19 in addition.

(B) When binding of MIP18 to MMS19 is impaired or in a situation when MMS19 levels are low, MIP18 is no longer protected by MMS19 and gets targeted for proteasomal degradation.




Europe PMC Funders Author Manuscripts